HEPES, 10 glucose, pH 7.4 (see equation (2)[30]).

$$P_X/P_{Na} = \{[Na^+]_o/[X]_o\}\{\exp((F/RT)(V_X - V_{Na}))\} \quad (1)$$

$$P_{Ca}/P_{Na} = \{[Na^+]_o/4[Ca^{2+}]_o\}\{\exp((F/RT)(V_{Ca} - V_{Na}))\}\{1 + \exp(FV_{Ca}/RT)\} \quad (2)$$

where $[X]_o$ is defined as the extracellular concentration of the given ion, P is defined as the permeability of the ion indicated by the subscript, F is Faraday's constant, R is the gas constant, T is absolute temperature and V is the reversal potential for the ion indicated by the subscript.

Calcium imaging

Cells were loaded with 2 μM Fura-2 AM in cell culture medium at room temperature for 30 min. We recorded Fura-2 ratios (F340/F380) on a MERLIN imaging system (Olympus). The standard curve for Fura-2 ratio versus Ca^{2+} concentration was constructed using the Fura-2 calcium imaging calibration kit (Molecular Probes).

Data analysis

Group data are presented as mean ± s.e.m. Statistical comparisons were made using analysis of variance and the *t*-test with Bonferroni correction. A two-tailed value of $P < 0.05$ was taken to be statistically significant.

Received 26 April; accepted 28 May 2002; doi:10.1038/nature00882.
Published online 23 June 2002; corrected 11 July (details online).

1. Caterina, M. J. *et al.* The capsaicin receptor: a heat-activated ion channel in the pain pathway. *Nature* **389,** 816–824 (1997).
2. Caterina, M. J., Rosen, T. A., Tominaga, M., Brake, A. J. & Julius, D. A capsaicin-receptor homologue with a high threshold for noxious heat. *Nature* **398,** 436–441 (1999).
3. McKemy, D. D., Neuhausser, W. M. & Julius, D. Identification of a cold receptor reveals a general role for TRP channels in thermosensation. *Nature* **416,** 52–58 (2002).
4. Peier, A. M. *et al.* A TRP channel that senses cold stimuli and menthol. *Cell* **108,** 705–715 (2002).
5. Spray, D. C. Cutaneous temperature receptors. *Annu. Rev. Physiol.* **48,** 625–638 (1986).
6. Reichling, D. B. & Levine, J. D. Heat transduction in rat sensory neurons by calcium-dependent activation of a cation channel. *Proc. Natl Acad. Sci. USA* **94,** 7006–7011 (1997).
7. Gotoh, H., Akatsuka, H. & Suto, K. Warm cells revealed by microfluorimetry of Ca^{2+} in cultured dorsal root ganglion neurons. *Brain Res.* **796,** 319–322 (1998).
8. Cesare, P., Moriondo, A., Vellani, V. & McNaughton, P. A. Ion channels gated by heat. *Proc. Natl Acad. Sci. USA* **96,** 7658–7663 (1999).
9. Hori, A., Minato, K. & Kobayashi, S. Warming-activated channels of warm-sensitive neurons in rat hypothalamic slices. *Neurosci. Lett.* **275,** 93–96 (1999).
10. Liu, L. & Simon, S. A. Capsaicin, acid and heat-evoked currents in rat trigeminal ganglion neurons; relationship to functional VR1 receptors. *Physiol. Behav.* **69,** 363–378 (2000).
11. Brengelmann, G. L. in *Textbook of Physiology Volume 2: Circulation, Respiration, Body Fluids, Metabolism, and Endocrinology* (eds Patton, H. D., Fuchs, A. F., Hille, B., Scher, A. M. & Steiner, R.) 1584–1596, (W.B. Saunders, Philadelphia, 1989).
12. Hille, B. *Ion Channels of Excitable Membranes* (Sinauer Associates, Sunderland, Massachusetts, 2001).
13. Möller, S., Croning, M. D. & Apweiler, R. Evaluation of methods for the prediction of membrane spanning regions. *Bioinformatics* **17,** 646–653 (2001).
14. Tominaga, M. *et al.* The cloned capsaicin receptor integrates multiple pain-producing stimuli. *Neuron* **21,** 531–543 (1998).
15. Fundin, B. T., Rice, F. L., Pfaller, K. & Arvidsson, J. The innervation of the mystacial pad in the adult rat studied by anterograde transport of HRP conjugates. *Exp. Brain Res.* **99,** 233–246 (1994).
16. Kanzaki, M. *et al.* Translocation of a calcium-permeable cation channel induced by insulin-like growth factor-1. *Nature Cell. Biol.* **1,** 165–170 (1999).
17. Liedtke, W. *et al.* Vanilloid receptor-related osmotically activated channel (VR-OAC), a candidate vertebrate osmoreceptor. *Cell* **103,** 525–535 (2000).
18. Strotmann, R., Harteneck, C., Nunnenmacher, K., Schultz, G. & Plant, T. D. OTRPC4, a nonselective cation channel that confers sensitivity to extracellular osmolarity. *Nature Cell Biol.* **2,** 695–702 (2000).
19. Watanabe, H. *et al.* Activation of TRPV4 channels (hVRL-2/mTRP12) by phorbol derivatives. *J. Biol. Chem.* **4,** 13569–13577 (2002).
20. Prakriya, M. & Lewis, R. S. Separation and characterization of currents through store-operated CRAC channels and Mg^{2+}-inhibited cation (MIC) channels. *J. Gen. Physiol.* **119,** 487–508 (2002).
21. Nadler, M. J. *et al.* LTRPC7 is a Mg·ATP-regulated divalent cation channel required for cell viability. *Nature* **411,** 590–595 (2001).
22. Runnels, L. W., Yue, L. & Clapham, D. E. TRP-PLIK, a bifunctional protein with kinase and ion channel activities. *Science* **291,** 1043–1047 (2001).
23. Jordt, S. E. & Julius, D. Molecular basis for species-specific sensitivity to 'hot' chili peppers. *Cell* **108,** 421–430 (2002).
24. DeCoursey, T. E. & Cherny, V. V. Temperature dependence of voltage-gated H^+ currents in human neutrophils, rat alveolar epithelial cells, and mammalian phagocytes. *J. Gen. Physiol.* **112,** 503–522 (1998).
25. Davis, J. B. *et al.* Vanilloid receptor-1 is essential for inflammatory thermal hyperalgesia. *Nature* **405,** 183–187 (2000).
26. Vyklicky, L. *et al.* Temperature coefficient of membrane currents induced by noxious heat in sensory neurones in the rat. *J. Physiol.* **517,** 181–192 (1999).
27. Andrew, D. & Craig, A. D. Spinothalamic lamina I neurones selectively responsive to cutaneous warming in cats. *J. Physiol.* **537,** 489–495 (2001).
28. Nagy, I. & Rang, H. P. Similarities and differences between the responses of rat sensory neurons to noxious heat and capsaicin. *J. Neurosci.* **19,** 10647–10655 (1999).
29. Qu, Y. *et al.* Differential modulation of sodium channel gating and persistent sodium currents by the β1, β2, and β3 subunits. *Mol. Cell Neurosci.* **18,** 570–580 (2001).
30. Lewis, C. A. Ion-concentration dependence of the reversal potential and the single channel conductance of ion channels at the frog neuromuscular junction. *J. Physiol.* **286,** 417–445 (1979).

Supplementary Information accompanies the paper on *Nature*'s website (http://www.nature.com/nature).

Acknowledgements

We thank U. Berger, L. Yue, X. Wei, W. Yu, A. Kabakov, L. Runnels, J. Pulido, W. Cao and H. Ferriera for assistance. We are grateful to S. Glucksmann, O. Tayber, L. DeFelice and members of Clapham laboratory for discussion and comments.

Competing interests statement

The authors declare competing financial interests: details accompany the paper on *Nature*'s website (http://www.nature.com/nature).

Correspondence and requests for materials should be addressed to D.E.C. (e-mail: dclapham@enders.tch.harvard.edu). Sequences have been deposited in GenBank under accession number AF514998 (hTRPV3).

TRPV3 is a temperature-sensitive vanilloid receptor-like protein

G. D. Smith*†, M. J. Gunthorpe*†, R. E. Kelsell‡, P. D. Hayes‡, P. Reilly*, P. Facer§, J. E. Wright*, J. C. Jerman‖, J.-P. Walhin‡, L. Ooi*, J. Egerton*, K. J. Charles*, D. Smart*, A. D. Randall*, P. Anand§ & J. B. Davis*

** Neurology-CEDD, ‡ Genetics Research, and ‖ Discovery Research, GlaxoSmithKline, Third Avenue, Harlow CM19 5AW, UK*
§ Peripheral Neuropathy Unit, Imperial College, Hammersmith Hospital, Du Cane Rd, London W12 0NN, UK
† These authors contributed equally to this work

Vanilloid receptor-1 (VR1, also known as TRPV1) is a thermosensitive, nonselective cation channel that is expressed by capsaicin-sensitive sensory afferents and is activated by noxious heat, acidic pH and the alkaloid irritant capsaicin[1]. Although *VR1* gene disruption results in a loss of capsaicin responses, it has minimal effects on thermal nociception[2,3]. This and other experiments—such as those showing the existence of capsaicin-insensitive heat sensors in sensory neurons[4]—suggest the existence of thermosensitive receptors distinct from VR1. Here we identify a member of the vanilloid receptor/*TRP* gene family, vanilloid receptor-like protein 3 (VRL3, also known as TRPV3), which is heat-sensitive but capsaicin-insensitive. VRL3 is coded for by a 2,370-base-pair open reading frame, transcribed from a gene adjacent to *VR1*, and is structurally homologous to VR1. VRL3 responds to noxious heat with a threshold of about 39 °C and is co-expressed in dorsal root ganglion neurons with VR1. Furthermore, when heterologously expressed, VRL3 is able to associate with VR1 and may modulate its responses. Hence, not only is VRL3 a thermosensitive ion channel but it may represent an additional vanilloid receptor subunit involved in the formation of heteromeric vanilloid receptor channels.

On the basis of the reasoning that a family of thermoreceptors homologous to VR1 might exist, we searched public nucleotide databases for sequences homologous to those of vanilloid receptor family members. Because we had previously noted that two members of this family, TRPV6/CaT1 (ref. 5) and TRPV5/ECAC1 (ref. 6), were co-localized on chromosome 7 (ref. 7), we focused our searches in genomic regions flanking TRPV1/VR1 17p13 (ref. 8) and TRPV4/VRL-2 12q23-24.1 (ref. 9). Sequence searches of the GenBank database led to the identification of an unfinished human genomic sequence (AC025125) sharing homology with human VR1 (AJ277028). Polymerase chain reaction (PCR) and rapid amplification of complementary DNA ends (RACE) analyses were used to extend the partial gene prediction. Analysis of the sequences

revealed a new vanilloid receptor-like protein, which we refer to as vanilloid receptor-like protein 3 (VRL3), and may be nominated as *TRPV3* in the newly defined *TRP* gene nomenclature[10]. A partial, homologous sequence without an ascribed function has been noted previously by ref. 11. Analysis of the longest version of human (h)*VRL3* indicated that, similar to *hVR1*, it is divided into 17 coding exons and one upstream non-coding exon (Fig. 1a). By linking the sequenced tagged site (STS) sequences G54317, G54316, G54321 and G54306 to AC025125—the genomic sequence first identified in our searches—*VRL3* was mapped to chromosome 17p13, which is close to *VR1* (ref. 12). The most 5′ sequence of *VRL3* obtained and the most 3′ region of *VR1* coincided on one fragment of AC027796, placing the two genes only ~7.5 kb apart and in the same transcriptional orientation (Fig. 1a). It remains to be determined whether their transcription is co-regulated; however, the juxtapositioning of *VR1* and *VRL3* provides further evidence of gene duplication events during the evolution of these channels and raises the likelihood of the genes having similar functional properties[7].

The complete hVRL3 open reading frame (ORF) of 2,370 bp codes for a polypeptide of 790 amino acids (Fig. 1b) with 43%, 42%, 41% and 30% identity to TRPV1/hVR1 (ref. 8), TRPV4/hVRL-2 (ref. 13), TRPV2/hVRL-1 (ref. 14) and TRPV6/hCaT1 (ref. 5) or TRPV5/hECAC[6], respectively (see Supplementary Information for alignment). The predicted structure of the protein encompasses a number of features present in VR1 including cytoplasmic termini, ankyrin domains, six transmembrane segments and a pore re-entrant loop, along with several putative phosphorylation sites (Fig. 1b). During amplification of the cDNA, a number of splice variants matching the genomic exon/intron structure were identified; the functional consequences and expression patterns of these splice forms remains to be determined.

VR1 is a polymodal receptor activated by capsaicin, by pH of less than ~6.0 and heat greater than ~42 °C, whereas VRL-1 is activated by heat alone[14]. Using electrophysiological and fluorometric techniques applied to HEK293 cells transiently transfected with hVRL3 we examined whether VRL3 possessed a similar activation profile to VR1. In both types of assay VRL3 consistently failed to respond to capsaicin or any other chemical activator of VR1, including extracellular acidification, even at concentrations maximal for VR1 activation (Fig. 2a). In contrast, mild heat challenges evoked currents in VR1 (Fig. 2b) and in approximately 70% of cells transfected with VRL3 (Fig. 2c; $n = 21$). As described previously[8], untransfected or mock-transfected HEK293 cells only exhibit small 'physicochemically mediated' heat-activated currents (0–40 pA over 25–48 °C, $n = 4$), which are not associated with increased current variance and are linearly related to temperature (Fig. 2b, c). Temperature response curves for VRL3 and VR1 current established that VRL3 has a marked threshold for activation at ~39 °C (Fig. 2c), compared with ~42 °C for VR1 (Fig. 2b), and gives rise to substantial currents at higher temperatures (303 ± 134 pA at 50 °C, $n = 5$) in VRL3 transfected cells. VR1 currents were typically fully activated within ~500 ms, whereas VRL3 currents exhibited slower kinetics and peaked within ~2 s. The VRL3-mediated currents were always associated with an increase in current noise (Fig. 2c), which was analysed (variance analysis) to estimate the current carried by the unitary events. Unitary currents were estimated to be −1.53 ± 0.21 pA and −3.33 ± 0.25 pA ($n = 5$, $P < 0.001$), yielding conductance estimates of 21.9 ± 3.0 pS and 47.6 ± 3.6 pS for VR1 and VRL3 respectively, under identical recording conditions at 48–50 °C. Thus VRL3 has a conductance similar to other TRPV family members[15] but apparently at a level twofold greater than VR1; however, this difference may be modified, such as by the effect of divalent ions.

Current–voltage relationships were established for heat-gated VRL3-mediated currents (Fig. 2d) and found to be similar to that for VR1 (refs 1, 8), exhibiting a reversal potential close to 0 mV ($E_{rev} = -3.8 \pm 2.2$ mV, $n = 3$) and pronounced outward rectification ($I_{+70\,mV}/I_{-70\,mV} = 6.8 \pm 1.7$, $n = 3$). Ruthenium red, a non-selective TRPV channel blocker[15], reversibly inhibited (75 ± 9% inhibition, $n = 4$) hVRL3 heat-gated currents (Fig. 2e), similar to its effect on VR1 (79 ± 5% inhibition, $n = 3$; data not shown). Capsazepine, a tool antagonist of VR1 (ref. 8, 15), did not inhibit VRL3 (Fig. 2f).

We measured VRL3 messenger RNA expression in human tissues by Taqman quantitative PCR (Fig. 3a). *VRL3* was abundantly expressed in the central nervous system (CNS) with lower levels in peripheral tissues, suggesting that it is predominantly a gene of the nervous system. Target-specific polyclonal antisera to hVRL3 and hVR1 were used to investigate expression in human dorsal root ganglia (DRG). Both VRL3- and VR1-immunoreactive neurons were scattered throughout control DRG, although VRL3 appeared in fewer cells than VR1. Strong VRL3 immunoreactivity was found

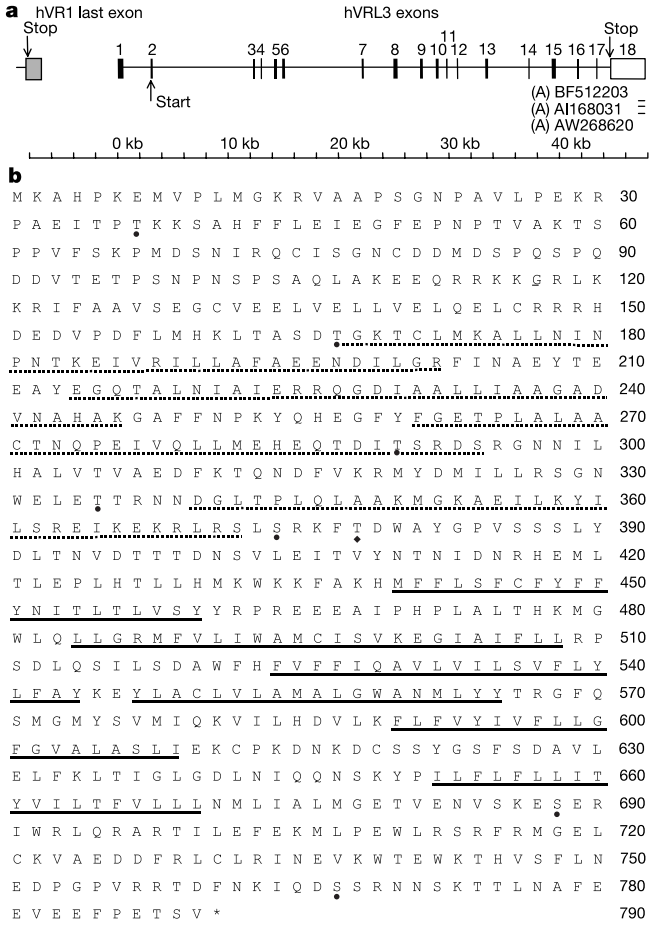

Figure 1 Genomic and protein structure of hVRL3. **a**, Genomic structure and proximity of *hVRL3* to *hVR1*. *hVRL3* extends over approximately 48 kb (see scale bar). Exons in black represent experimentally verified sequences. Exon 18 of *hVRL3* is extended (indicated by open box) by the expressed sequence tags (ESTs) indicated, which contain a polyadenylation signal also preserved in the genomic sequence (indicated by (A)). The *VRL3* translation start and stop sites and last exon of *VR1* are indicated three base pairs into exon 2, 93 bp into the last exon and 7.5 kb upstream of *hVRL3* (in grey), respectively. **b**, Polypeptide sequence of human VRL3. Amino acid residues are numbered in the margin. Ankyrin repeat domains (dashed lines) and hydrophobic regions representing transmembrane domains 1–6 (solid lines) were predicted using SMART[27] and TMPRED[28]; consensus sites for protein kinase A (filled diamond) and protein kinase C (filled circles) are shown. On the basis of the structure of other family members, the pore loop region is presumed to be situated between transmembrane domains 5 and 6.

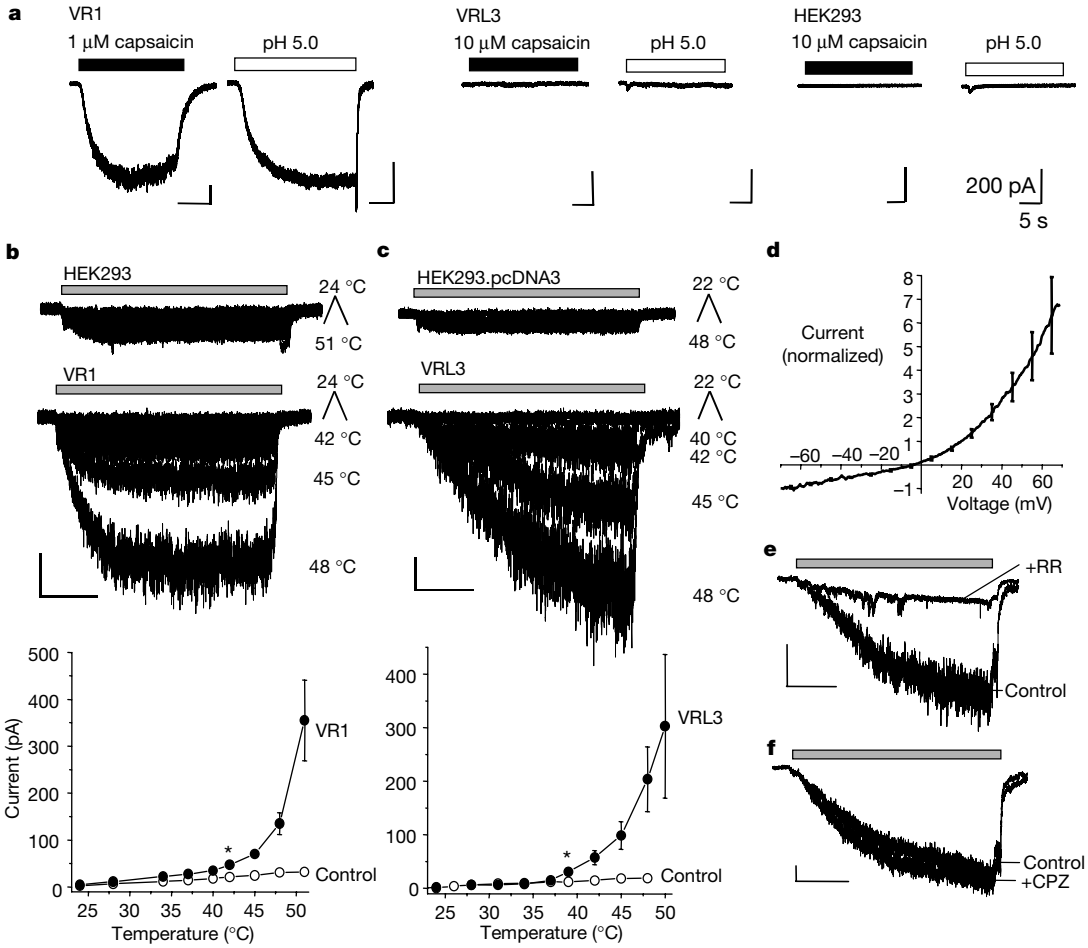

Figure 2 Activation of hVR1 and hVRL3 by noxious heat, capsaicin or protons. **a**, Whole-cell patch clamp recordings of membrane currents in VR1-, VRL3-transfected or untransfected HEK293 cells exposed to capsaicin or pH 5.0. Robust responses were seen with VR1 (1 μM capsaicin, 803 ± 96 pA, $n = 6$; pH 5.0, 460 ± 83 pA, $n = 6$). **b**, **c**, Whole-cell patch clamp recordings of membrane currents in control cells (top panels) and hVR1- (**b**) or hVRL3-transfected (**c**) cells (middle panels) recorded in response to the application of extracellular solutions over the temperature range indicated. Temperature-response curves are shown in the bottom panels (filled circles, $n = 4$–6 for all temperature points shown). Statistical significance (asterisk, $P < 0.05$) at temperatures ≥42 °C compared with control for VR1 and ≥39 °C compared with control for VRL3 are indicated. **d**, Current–voltage relationship for hVRL3 gated at 50–53 °C. Net current was ascertained by subtraction of control data recorded at 23–25 °C ($n = 3$). **e**, **f**, Antagonism of VRL3 currents evoked by 50–52 °C heat. Ruthenium red (RR, 10 μM) blocks (75 ± 9% inhibition, $n = 4$) VRL3 currents (**e**); however, capsazepine (CPZ, 10 μM) does not (**f**). Scale bars: **a**, all 200 pA (vertical), 5 s (horizontal); **b**, 100 pA, 500 ms; **c**, 100 pA, 500 ms; **e**, 250 pA, 500 ms; **f**, 200 pA, 500 ms.

in cells with a diameter ≤50 μm (Fig. 3b) and much weaker immunoreactivity in a few (about 10% of the total) larger (>50 μm) cells. Serial sections showed that VRL3 and VR1 immunoreactivities were localized together in sensory neurons (Fig. 3b, c). VRL3 or VR1 immunoreactivity was completely abolished by preabsorption with their respective antigens (Fig. 3d). In avulsed DRG, the number of cells with diameter ≤50 μm that were immunoreactive was increased significantly for both VRL3 and VR1 in comparison with age-matched controls (Fig. 3e). Counts of either VRL3 or VR1 immunoreactive cells with a diameter of greater than 50 μm showed no change after injury. No correlation was detected between surgical delay or age of subject, or between the number of VRL3 or VR1 immunoreactive cells in control or injured DRG.

One aspect of vanilloid receptor physiology that has not been fully explored to date is the occurrence of heteromeric channel assemblies, as observed for P2X[16] or ASIC[17] ion channels. Their shared chromosomal co-localization, co-expression in neurons, and heat-mediated gating suggests that VR1 and VRL3 may be ideal candidates for intrafamily heteromerization. To test this hypothesis, VRL3 was tagged with an Myc epitope to facilitate immunoprecipitation, and immunoprecipitated from HEK293 cells co-transfected with VR1 and VRL3. VR1 was co-precipitated (Fig. 4a top panel) in a fashion that was dependent on the presence of VRL3 in the immune complex. Similarly, precipitation of VR1 was found to co-precipitate VRL3 (Fig. 4a second panel), which was not due to nonspecific interactions with the supports, Myc tag or precipitating antibody.

Elevating the expression of a channel subunit and changing channel subunit composition may be a control mechanism in afferent activation, possibly operating through alteration of ion channel biophysics and/or pharmacology. To study whether the presence of VRL3 affects the functional properties of VR1, cells were co-transfected with VR1, plus either vector control or VRL3, and the VR1 response then measured by monitoring intracellular calcium. Cells transfected with VR1 alone responded to capsaicin or protons, whereas cells transfected with VRL3 alone failed to respond to either ligand (Fig. 4b, c). Co-expression of VRL3 with VR1 produced a substantial increase in the response to capsaicin (Fig. 4b) and a similar increase in the response to protons (Fig. 4c). Capsazepine was able to block the response of VR1 and VRL3 co-transfected cells to capsaicin or protons with no increase in

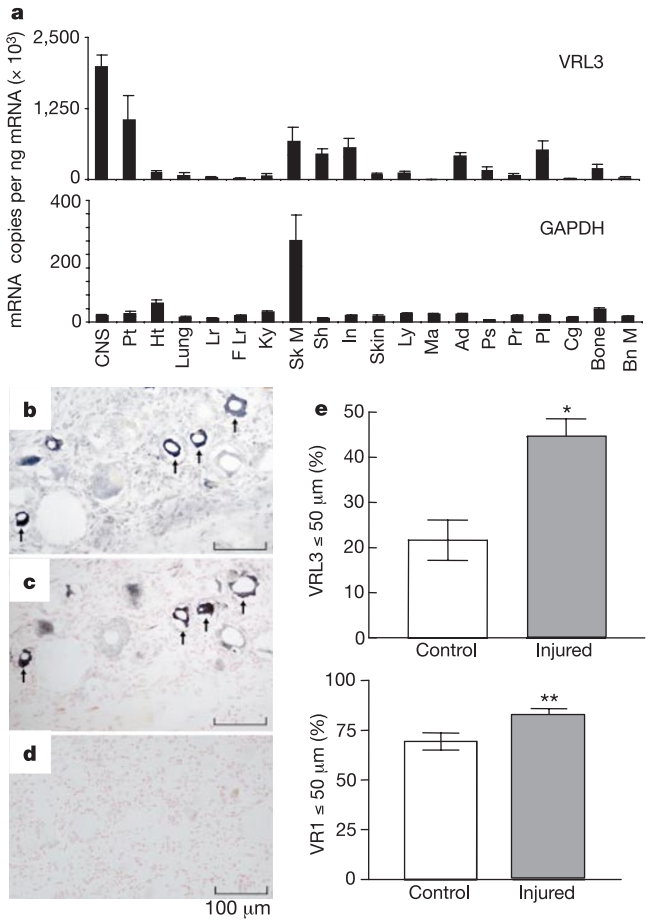

Figure 3 Localization of VRL3. **a**, mRNA expression of hVRL3 in human tissues. Copies of hVRL3 (top) or GAPDH (bottom) per 50 ng total RNA ($n = 4$, mean ± s.e.m.). Pt, pituitary; Ht, heart; Lr, liver; F Lr, fetal liver; Ky, kidney; Sk M, skeletal muscle; Sh, stomach; In, intestine; Ly, lymphocytes; Ma, macrophages; As, adipose; Ps, pancreas; Pr, prostate; Pl, placenta; Cg, cartilage; Bn M, bone marrow. **b**, **c**, Serial, human DRG sections immunostained with antibodies to hVRL3 (**b**) or hVR1 (**c**) showing the same cells immunoreactive for both antigens (arrows). **d**, DRG sections immunostained with antibodies pre-incubated with homologous antigen to hVRL3. Scale bars, 100 μm. **e**, Quantification of VRL3- and VR1-immunoreactivity in neurons from control or injured DRG. Bar charts show a significant increase in the number of immunoreactive cells after injury. VRL3: asterisk, $P = 0.0025$; VR1: double asterisk, $P = 0.015$ (Student's *t*-test).

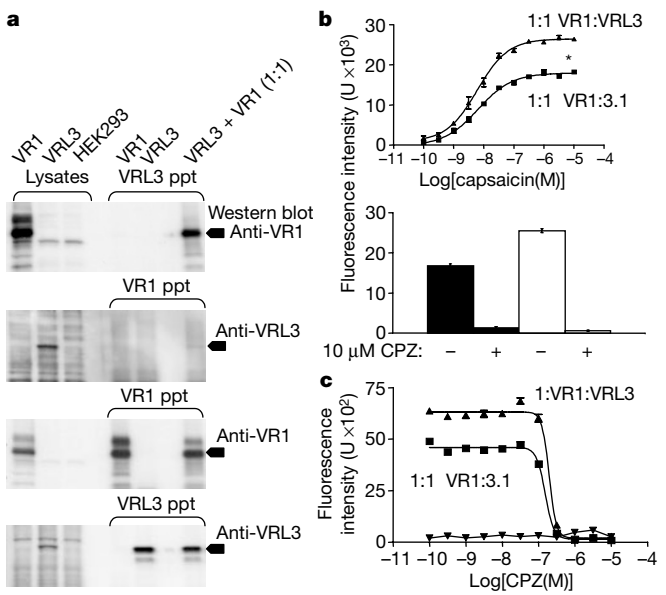

Figure 4 Association between VR1 and VRL3. **a**, Co-precipitation of VR1 and VRL3. Lysates from HEK293 cells co-transfected with VR1 and VRL3-Myc or vector were analysed by western blot before or after affinity purification using C22 or anti-Myc antibodies to precipitate VR1 or VRL3-Myc, respectively. VR1 co-precipitated with VRL3-Myc (top panel) and hVRL3-Myc co-precipitated with VR1 (second panel, shown by arrows). **b**, Enhancement of VR1 response to capsaicin by co-expression with VRL3 (upper panel). HEK293 cells co-transfected with VR1 plus vector control (squares) or VR1 plus hVRL3 (triangles) were challenged with the capsaicin concentrations shown (asterisk, $P < 0.0001$, $n = 4$). Capsazepine (CPZ, 10 μM) antagonized the response to 100 nM capsaicin of cells co-transfected with VR1 plus vector control (black bars) or VR1 plus VRL3 (white bars, bottom panel). **c**, The enhanced response of VR1 (squares) to protons (pH 5.0) when co-transfected with VRL3 (triangles) and the inhibition of the response by CPZ 10 μM are shown. Changes in intracellular calcium were expressed as mean change of peak minus basal fluorescence intensity ± s.e.m. ($n = 4$). ppt, precipitation.

residual activity compared to VR1 transfected cells, suggesting that capsazepine is equally able to block any VR1–VRL3 heteromeric channels formed. This data suggests that VRL3 may contribute to VR1 responses by a mechanism that might, given the evidence for interaction described above, entail formation of heteromeric channels. At this stage, however, we cannot rule out that the functional effect might occur as a result of alterations in VR1 transport or competition for desensitizing mechanisms.

Although additional TRPV family members have been identified, none of the functional properties of the previously identified paralogues provide a complete explanation for heat responses in capsaicin-insensitive neurons[4] or the thermal nociception remaining in VR1 knockout mice[2,3]. In contrast to TRPV2/VRL-1 (heat threshold ~52 °C), VRL3 responds in a similar temperature range to VR1 and is a candidate for the 'unexplained' heat sensor of VR1 knockout mice. It is unclear then why VRL3 activity was not detected in the neonatal sensory neurons of *VR1* knockout mice[2,3]. This may be a consequence of the age of ganglia dissected or the chosen culture conditions, as previously suggested[3]. Another possibility is that the *VR1* knockout strategies have deleted transcriptional control elements shared between *VR1* and *VRL3*. These considerations lead to the possibility that *VRL3* disruption contributed to the phenotype ascribed to disruption of *VR1* and also to the possible existence of yet further thermal receptors—questions which may be answered by VRL3 and VR1 knockout studies.

The observations of co-expression of VRL3 and VR1 in individual sensory neurons and the biochemical evidence for association between the two proteins, gives rise to a hypothesis that VRL3, or possibly other TRP proteins, may contribute subunits to vanilloid receptor-like ion channels. Such heteromerization may allow sensory neurons to express a range of receptors with a spectrum of response characteristics wider than those of the individual homomeric receptors. Thus, the identification of VRL3 and its different threshold and kinetic characteristics compared to VR1 supports the view that members of the TRPV family may constitute a family of thermal sensors that code for a dynamic range of thermal sensitivity in sensory neurons[14]. A further development, however, is that differential regulation of *TRPV* expression, or the formation of heteromeric interactions, may underlie the thermal hypersensitivity of sensory neurons at sites of tissue injury and inflammation. □

Methods

Cloning of cDNA for hVRL3

Homology searching and gene predictions were performed using TBLASTN2 (ref. 18), GENEWISE[19] and GENSCAN[20] programs. All other general sequence manipulations were performed with GCG version 9 and 10.2 (Genetics Computer Group Inc). We conducted

cDNA cloning using previously described methods[8]. Primers derived from the *hVRL3* gene prediction sequences were used to amplify cDNAs corresponding to the central part and the 3′ end by PCR with reverse transcription (RT–PCR) from brain, heart and testis poly(A)$^+$ RNA (Clontech). RACE was performed with small intestine, colon and bladder poly(A)$^+$ RNAs using the SMART RACE kit (Clontech). It was necessary to include 10% DMSO in the RACE reactions because of the high G + C content of the 5′ end. The complete coding region of the hVRL3 cDNA was amplified from small intestine and colon cDNAs by nested PCR using, for the primary reaction, forward 5′-TTGCCACGACCA CCCAGAAC-3′ and reverse 5′-CAGACGGCTGCTGGCTGTAG-3′ primers, and for the secondary reaction, forward 5′-ACCATGAAAGCCCACCCCAAG-3′ and reverse 5′-TCTCTGCACAGAGTCGGTGAC-3′ primers. Multiple full-length cDNA clones, from independent PCR reactions, were double-strand-sequenced to rule out PCR-introduced mutations.

Electrophysiology

HEK293 cells were cultured and transiently transfected with pcDNA3.1-hVR1 or pcDNA3.1-hVRL3 and pIRES-GFP, prepared on coverslips, and whole-cell patch-clamp recordings were performed as previously described[8]. Experiments were conducted at room temperature (20–24 °C) unless otherwise stated. The extracellular solution consisted of (in mM): NaCl 130, KCl 5, $CaCl_2$ 2, $MgCl_2$ 1, glucose 30, HEPES-NaOH 25, pH 7.3. Patch pipettes (resistance 2–5 MΩ) were filled with the following solution (in mM): CsCl 140, $MgCl_2$ 4, EGTA 10, HEPES-CsOH 10, pH 7.3. Application of drugs and temperature jumps were applied using an automated device for fast switching of solutions coupled with an in-line heating device (Warner Instruments in-line heater SH-27A) as described[8]. Antagonists were pre-applied for at least 30 s. Data were acquired at 4 kHz and filtered at 2 kHz, and analysis was performed using the pClamp7 software suite and Origin (Microcal). Variance (noise) analysis was conducted as described[21]. All data are presented as the mean ± s.e.m.

Calcium imaging

Changes in intracellular calcium were monitored using a fluorometric imaging plate reader (FLIPR) platform as previously described[22]. Briefly, HEK293 cells transiently transfected with pcDNA3.1-hVRL3, pcDNA3.1-hVR1, vector alone or combinations of vectors, were plated into black-walled microtitre plates, loaded with the calcium indicator dye Fluo3 AM, and assayed as described[22]. Data are expressed as mean ± s.e.m. unless otherwise stated. Curve-fitting and parameter estimation were carried out using Graph Pad Prism 3.00 (GraphPad Software Inc). Statistical comparisons were made where appropriate using Student's *t*-test.

Localization studies

Tissue expression of human VRL3 was studied using Taqman quantitative RT–PCR[23] with 5′-CAAGGTCATCCATGACAACTTTG-3′ and 5′-GGGCCATCCACAGTCTTCTG-3′ primers in combination with a 5′-ACCACAGTCCATGCCATCACTGCCA-3′ probe for GAPDH, or 5′-CCTCCTCAACATGCTCATTGCT-3′ and 5′-ATGCGTTCGCTCT CCTTGG-3′ primers with a 5′-CGTTCTCCACAGTCTCGCCCATCA-3′ probe for VRL3, as previously described[24]. Data is presented as the mean number of copies per 50 ng of total RNA from four patients ± s.e.m. Samples were provided by the Netherlands Brain Bank. For immunohistochemical studies, cervical DRG whose roots had been avulsed from the spinal cord after traumatic injury to the brachial plexus were collected from ten adult patients during surgical repair—the delay between injury and collection of DRG at operation ranged from 1 to 74 days. Matched control cervical DRG were obtained through the Netherlands Brain Bank from six subjects with an autopsy delay of less than 12 h. All non-autopsy tissues were removed as a necessary part of surgical repair and not for research purposes; the patients gave informed consent for this study, which had local ethics committee approval. Tissues were stored, sectioned, post-fixed, counterstained and immunoreactivity detected as previously described[25]. Rabbit polyclonal antibodies C22 and N63, raised to a carboxy terminus peptide from human VR1 ((C)KPEDAEVFKSPAASGEK) and an amino-terminal peptide from VRL3 (LAKEEQRRKKG(C)), respectively, were used as primary antibodies. For co-localization, serial, inverted 'mirror image', frozen sections were collected and treated in the same fashion. Negative controls included omission of primary antibodies, replacement with pre-immune serum or pre-adsorption of antibodies with antigen. Nucleated, immunoreactive and non-immunoreactive DRG neurons were counted (140 ± 24 per control or 94 ± 14 per injured patient stained for VRL3; 170 ± 8 per control or 154 ± 14 per injured patient stained for VR1) and an approximation of cell diameter obtained using a calibrated microscope eyepiece graticule at × 20 objective magnification. Counts were made by two independent observers.

Immunoprecipitation

An Myc tag was placed at the C terminus of VRL3 using standard cDNA cloning procedures. HEK293 cells were transfected with VR1 or VRL3-Myc as described[8]. Transfected cells were lysed in 2 ml RIPA buffer (20 mM sodium phosphate pH 7.4, 500 mM NaCl, 0.1% SDS, 1% NP-40, 0.5% sodium deoxycholate) containing protease inhibitors (Complete, protease inhibitor cocktail tablets; Roche). Protein complexes were precipitated from pre-cleared lysates of equivalent protein content overnight at 4 °C using anti-Myc clone JAC6 (Serotec) (4 μg) or anti-VR1 antiserum (C22) (4 μg) and protein-A/Sepharose beads, washed with ice cold RIPA buffer and analysed by SDS–polyacrylamide gel electrophoresis and western blot essentially as described[26]. VR1 or VRL-3-Myc were detected using antiserum C22 (1:5,000) or anti-Myc-horseradish peroxidase (HRP) (Invitrogen) and HRP-conjugated donkey anti-rabbit (Sigma) where necessary, followed by detection by chemiluminescence. Myc-tagged proteins unrelated to VR1, such as neuropilin and human γ-2 calcium channel subunit were used as negative controls to show that association did not occur through the Myc tag. Furthermore, precipitation did not occur when lysates from singly transfected cells were mixed before precipitation, indicating that the VR1–VRL3 association must occur in the cell.

Received 21 February; accepted 29 May 2002; doi:10.1038/nature00894.
Published online 23 June 2002.

1. Caterina, M. J. *et al.* The capsaicin receptor: a heat-activated ion channel in the pain pathway. *Nature* **389,** 816–824 (1997).
2. Caterina, M. J. *et al.* Impaired nociception and pain sensation in mice lacking the capsaicin receptor. *Science* **288,** 306–313 (2000).
3. Davis, J. B. *et al.* Vanilloid receptor-1 is essential for inflammatory thermal hyperalgesia. *Nature* **405,** 183–187 (2000).
4. Nagy, I. & Rang, H. P. Similarities and differences between the responses of rat sensory neurons to noxious heat and capsaicin. *J. Neurosci.* **19,** 10647–10655 (1999).
5. Peng, J. B. *et al.* Human calcium transport protein CaT1. *Biochem. Biophys. Res. Commun.* **278,** 326–332 (2000).
6. Muller, D. *et al.* Molecular cloning, tissue distribution, and chromosomal mapping of the human epithelial Ca^{2+} channel (ECAC1). *Genomics* **67,** 48–53 (2001).
7. Muller, D. *et al.* Gene structure and chromosomal mapping of human epithelial calcium channel. *Biochem. Biophys. Res. Commun.* **275,** 47–52 (2000).
8. Hayes, P. D. *et al.* Cloning and functional expression of a human orthologue of rat vanilloid receptor-1. *Pain* **88,** 205–215 (2000).
9. Delany, N. S. *et al.* Identification and characterization of a novel human vanilloid receptor-like protein, VRL-2. *Physiol. Genom.* **4,** 165–174 (2001).
10. Montell, C. *et al.* A unified nomenclature for the superfamily of TRP cation channels. *Mol. Cell* **9,** 229–231 (2002).
11. Peng, J. B. *et al.* Structural conservation of the genes encoding CaT1, CaT2 and related cation channels. *Genomics* **76,** 99–109 (2001).
12. Touchman, J. W. *et al.* The genomic region encompassing the nephropathic cystinosis gene (CTNS): complete sequencing of a 200 kb segment and discovery of a novel gene within the common cystinosis-causing deletion. *Genome Res.* **10,** 165–173 (2000).
13. Liedtke, W. *et al.* Vanilloid receptor-related osmotically activated channel (VR-OAC), a candidate vertebrate osmoreceptor. *Cell* **103,** 525–535 (2000).
14. Caterina, M. J. *et al.* A capsaicin-receptor homologue with a high threshold for noxious heat. *Nature* **398,** 436–441 (1999).
15. Gunthorpe, M. J., Benham, C. D., Randall, A. & Davis, J. B. The diversity in the vanilloid (TRPV) receptor family of ion channels. *Trends Pharmacol. Sci.* **23,** 183–191 (2002).
16. Liu, M. *et al.* Coexpression of P2X(3) and P2X(2) receptor subunits in varying amounts generates heterologous populations of P2X receptors that evoke a spectrum of agonist responses comparable to that seen in sensory neurons. *J. Pharmacol. Exp. Ther.* **296,** 1043–1050 (2001).
17. Babinski, K., Catarsi, S., Biagini, G. & Seguela, P. Mammalian ASIC2a and ASIC3 subunits co-assemble into heteromeric proton-gated channels sensitive to Gd3 + . *J. Biol. Chem.* **275,** 28519–28525 (2000).
18. Altschul, S. F., Gish, W., Miller, W., Myers, E. W. & Lipman, D. J. Basic local alignment search tool. *J. Mol. Biol.* **215,** 403–410 (1990).
19. Birney, E. & Durbin, R. Using GeneWise in the *Drosophila* annotation experiment. *Genome Res.* **10,** 547–548 (2000).
20. Burge, C. & Karlin, S. Prediction of complete gene structures in human genomic DNA. *J. Mol. Biol.* **268,** 78–94 (1997).
21. Dempster, J. *Computer Analysis of Electrophysiological Signals* (Academic, London, 1993).
22. Smart, D. *et al.* The endogenous lipid anandamide is a full agonist at the human vanilloid receptor (hVR1). *Br. J. Pharmacol.* **129,** 227–230 (2000).
23. Gibson, U. E., Heid, C. A. & Williams, P. M. A novel method for real time quantitative RT-PCR. *Genome Res.* **6,** 995–1001 (1996).
24. Moore, D. J. *et al.* Expression pattern of human P2Y receptor subtypes: a quantitative reverse transcription-polymerase chain reaction study. *Biochim. Biophys. Acta* **1521,** 107–119 (2001).
25. Coward, K. *et al.* Immunolocalization of SNS/PN3 and NaN/SNS2 sodium channels in human pain states. *Pain* **85,** 41–50 (2000).
26. Gray, C. W. *et al.* Characterisation of human HtrA2, a novel serine protease involved in the mammalian cellular stress response. *Eur. J. Biochem.* **267,** 5699–5710 (2000).
27. Schultz, J., Milpetz, F., Bork, P. & Ponting, C. P. SMART, a simple modular architecture research tool: identification of signalling domains. *Proc. Natl Acad. Sci. USA* **95,** 5857–5864 (1998).
28. Hofmann, K. & Stoffel, W. TMbase—a database of membrane spanning proteins segments. *Biol. Chem. Hoppe-Seyler* **374,** 166 (1993).

Supplementary Information accompanies the paper on *Nature*'s website (http://www.nature.com/nature).

Acknowledgements

The authors acknowledge R. Birch and R. Ravid for supply of human adult tissues; I. Gloger, C. Benham, M. Duckworth and C. Bountra for advice and encouragement; and C. Farrant for help with artwork.

Competing interests statement

The authors declare competing financial interests: details accompany the paper on *Nature*'s website (http://www.nature.com/nature).

Correspondence and requests for materials should be addressed to J.B.D. (e-mail: John_B_Davis@gsk.com). The GenBank accession number for human VRL3 is AJ487035.

